Modal parameter identification for closely spaced modes using an Empirical Fourier decomposition-based method

Shimin Li[a,*], Yuelong Liu[a], Pengcheng Wang[b], Xian Li[c], Zhengwei Li[c]

[a]Guiyang Yunyan District Municipal Engineering Management Office, Guiyang, China

[b]Guizhou Construction Science Research & Design Institute Limited Company of CSCEC, Guiyang, China

[c]Guizhou Gongda Science and Technology Service Co. LTD, Guiyang, China

*Corresponding author: shiminli@hotmail.com; Tel: +086 18798082860.

Abstract: Precise and effective identification of modal parameters is important for a civil structure throughout the structural lifetime. A time-frequency method for modal parameter identification is developed based on a recently developed adaptive method for signal decomposition, i.e., empirical Fourier decomposition (EFD). The EFD is used to separate a multi-component free vibration response into the summation of several mono-component modal responses. The modal frequencies and modal damping ratios are calculated from the modal responses by using the empirical envelope method and a damping estimation method. Two numerical examples and one experimental example are provided to validate the EFD-based time-frequency method and highlight the improvements of the EFD-based method relative to the empirical mode decomposition (EMD)-based method. It is highlighted that the EFD-based method has a much higher frequency resolution and lower computational cost than the EMD-based method. Hence, the proposed EFD-based method is suitable for online modal parameter identifications of structures with closely spaced modes. In addition, the EFD-based method is useful for both linear and nonlinear systems.

Keywords: Modal parameter identification; Empirical Fourier decomposition (EFD); Closely spaced modes; Nonlinear system; Time-frequency method

1. Introduction

Modal parameter identification of a civil structure is important in various aspects including dynamic response assessment, structural health monitoring, vibration control, etc [1-6]. The important modal parameters for a specific structural mode include the natural frequency, the damping ratio, and the mode shape [7-10]. The modal parameters of a structure are often identified based on the vibration responses of the structure. According to the type of input, the vibration responses can be clarified into forced excitation-induced response, ambient excitation-induced response, and impulse excitation-induced response. It is usually unrealistic and unsafe to obtain reliable forced excitation-induced responses for a large-scale civil structure. The requirement for accurate measurement of the input force brings additional difficulties to the application of forced vibration-based modal parameter identifications. Therefore, output-only methods based on impulse or ambient excitation-induced responses have been largely investigated for modal parameter identifications of large civil structures. Classical output-only methods identify the modal parameters in the frequency domain or the time domain. Typical frequency-domain methods include the peak-picking method, the frequency-domain decomposition method, the frequency-spatial domain decomposition method, etc [11]. Typical time-domain methods include the random decrement technique, the autoregressive moving average method, the stochastic subspace identification method, etc [12, 13]. These classical time-domain methods and frequency-domain methods have achieved promising results for the identifications of linear systems. However, these classical methods are incapable of dealing with nonstationary vibrational responses and identifying the underlying nonlinear features of a practical structure. Recent efforts have been advanced for automated modal identification of different structures [14-18].

Time-frequency methods are drawing increasing attention in modal parameter identification because of the ability to identify the nonlinear and time-varying features of a structure. The short-time Fourier transform-based method and the wavelet transform-based method are among the earliest time-frequency methods [19]. However, the former is criticized due to the limited time-frequency resolution while the latter is criticized due to the difficulty to select an appropriate mother wavelet. More recently, the Hilbert-Huang transform-based method is proposed as an alternative time-frequency method [20]. The key part of the Hilbert-Huang transform-based method is the empirical mode decomposition (EMD) [20], which is an adaptive decomposition method to extract modal responses (mono-component signals) from vibrational responses (often multi-component signals). The Hilbert-Huang transform-based method and several variants have found applications in modal parameter identifications of bridges and tall buildings, etc [21-23].

Although the Hilbert-Huang transform-based method is promising for identifying nonlinear and time-varying systems, it is unable to identify a structure with closely spaced modes due to the limited frequency resolution of the EMD. More specifically, the intrinsic mode functions extracted by the EMD may include several closely spaced frequencies due to mode mixing [24]. Other shortcomings of the EMD include the end effects and the generated pseudo components with low energies and low frequencies [25]. Several improved versions (e.g., the ensemble EMD [26] and the complete ensemble EMD [27]) of EMD have been proposed to overcome these shortcomings. However, these improved EMD methods cannot fully avoid the mode mixing and end effects. Several different decomposition approaches with sound theoretical backgrounds

have also been proposed and utilized in modal parameter identifications, e.g., the variational mode decomposition [28] and the nonlinear mode decomposition [29]. However, these methods require large computational costs and hence they are not suitable for online modal parameter identification.

More recently, the empirical Fourier decomposition (EFD) [30] is proposed as a new adaptive decomposition method to overcome some shortcomings of existing adaptive decomposition methods. The EFD uses an adaptive segmentation technique to divide the Fourier spectrum of a multi-component signal and then constructs the mono-component signals based on a zero-phase filter bank and the inverse Fourier transform. Compared to the EMD, the EFD has higher frequency resolution and reduced end effects. The computational cost of the EFD is also low, and hence it is promising for online modal parameter identification. Zhou et al. [30] showed that the EFD can accurately decompose several types of multi-component signals; further, they showed that the EFD can calculate the instantaneous frequencies of the decomposed mono-component signals. However, the identifications of instantaneous damping ratios were not addressed. In addition, for typical civil structures (e.g., structures with closely spaced modes), the underlying superiorities of EFD in modal parameter identifications compared to existing time-frequency methods require further investigation.

Inspired by the improved capabilities of EFD in processing multi-component signals, this paper proposes an EFD-based time-frequency method for modal parameter (including modal frequency and damping ratio) identifications of systems with closely spaced modes. The superiorities of the proposed EFD-based method relative to the EMD-based method and several other methods are demonstrated by several numerical and experimental examples representing typical civil structures. The remainder of this paper is organized as follows. Starting with a brief introduction of the EFD in Section 2, the proposed EFD-based identification method is introduced in detail in Section 3. Two numerical examples and one experimental example are provided in Section 4 and Section 5 respectively to validate the EFD-based time-frequency method and highlight the improvements of the EFD-based method relative to the EMD-based method and several other methods. Some main conclusions are summarized in Section 6.

2. Empirical Fourier decomposition (EFD)

The vibrational (displacement, velocity, or acceleration) responses of a multiple-degree-of-freedom system are often multi-component signals. It is necessary to extract the modal responses (mono-component signals) from the multi-component signals in order to identify the modal parameters in the time-frequency domain. A free vibration response can be directly used to extract the modal responses. However, for an ambient vibration response, the signal should be processed (e.g., using the autocorrelation method or random decremental technique [31, 32]) to obtain the equivalent free vibration response. The multi-component free vibration response is then decomposed into the combination of several mono-component modal responses.

The decomposition of a multi-component signal can be described as follows

$$\mathrm{sig}(t)=\sum_{n=1}^{N}c_n(t)+\mathrm{noise}(t)=\sum_{n=1}^{N}A_n(t)\cos\left(\int\omega_n(t)\,dt+\varphi_n\right)+\mathrm{noise}(t) \tag{1}$$

where sig(t) is the multi-component vibrational signal; $c_k(t)$ (n = 1 ~ N) are the modal responses; N is the number of modal responses embedded in the vibrational signal; $A_n(t)$, $\omega_n(t)$, and φ_n represent the

instantaneous amplitude, the instantaneous frequency (in rad/s), and the initial phase of $c_n(t)$, respectively; noise(t) represents the measurement noise in the multi-component vibrational signal. The instantaneous frequency of $c_n(t)$ in Hz can be calculated as $f_n(t) = \omega_n(t)/(2\pi)$.

The EFD [30] normalizes the Fourier spectrum of sig(t) into a frequency range of $-\pi \sim \pi$. The Fourier spectrum is then divided by an improved segmentation technique and filtered into several frequency segments by a zero-phase filter bank. A mono-component signal is generated based on each frequency segment using the inverse Fourier transform. In the following parts of this section, the improved segmentation technique and the construction of the zero-phase filter bank are described for the frequency range $0 \sim \pi$. Those for the frequency range $-\pi \sim 0$ can be deduced based on the Hermitian symmetry of the Fourier spectrum.

In the improved segmentation technique, the frequency range is divided into N continuous frequency segments. The n^{th} ($n = 1 \sim N$) frequency segment is represented as $\omega_{n-1} \sim \omega_n$. To determine the values of ω_n, the local maxima of the Fourier spectrum are extracted into a series. The magnitudes at all local maxima and the Fourier spectrum magnitudes at $\omega = 0$ and $\omega = \pi$ are sorted in descending order. Frequencies corresponding to the first N largest Fourier spectrum magnitudes in the sorted series are represented as W_n ($n = 1 \sim N$). Furthermore, $W_0 = 0$ and $W_{N+1} = \pi$. The frequency range $0 \sim \pi$ is then divided into n segments with boundaries determined by

$$\omega_0 = \begin{cases} \arg\min \breve{X}\left(W_0 \sim W_1\right) & \text{if } W_0 \neq W_1 \\ W_0 & \text{if } W_0 = W_1 \end{cases} \tag{2a}$$

$$\omega_n = \operatorname{argmin} \breve{X}_n\left(\omega\right) \text{ for } n = 1 \sim \left(N-1\right) \tag{2b}$$

$$\omega_N = \begin{cases} \operatorname{argmin} \breve{X}\left(W_N \sim W_{N+1}\right) & \text{if } W_N \neq W_{N+1} \\ W_N & \text{if } W_N = W_{N+1} \end{cases} \tag{2c}$$

where $\operatorname{argmin} \breve{X}\left(W_0 \sim W_1\right)$ represents the frequency corresponding to the minimum spectrum magnitude in the frequency range $W_0 \sim W_1$; $\operatorname{argmin} \breve{X}_n\left(\omega\right)$ ($n = 1 \sim (N-1)$) represents the frequency corresponding to the minimum spectrum magnitude in the frequency range $W_n \sim W_{n+1}$; $\operatorname{argmin} \breve{X}\left(W_N \sim W_{N+1}\right)$ represents the frequency corresponding to the minimum spectrum magnitude in the frequency range $W_N \sim W_{N+1}$. The normalized Fourier spectrum of sig(t) is now divided into N segments using the improved segmentation technique described by Eq. (2).

A zero-phase filter bank is then constructed based on divided frequency segments. A zero-phase filter for a specific frequency segment is a band-pass filter with cut-off frequencies of ω_{n-1} and ω_n. Hence, the filter retains the component in the considered frequency segment while all other components are filtered out.

The Fourier transform of a signal sig(t) can be expressed as

$$\operatorname{sig}\left(\omega\right) = \int_{-\infty}^{\infty} \operatorname{sig}\left(t\right) e^{-j\omega t} dt \tag{3}$$

A zero-phase filter bank is constructed as

$$\hat{\mu}_n(\omega)=\begin{cases}1 & \text{if } \omega_{n-1}\le|\omega|\le\omega_n\\ 0 & \text{otherwise}\end{cases} \tag{4}$$

The resulting signal filtered by $\hat{\mu}_n(\omega)$ is

$$\hat{c}_n(\omega)=\hat{\mu}_n(\omega)\mathrm{sig}(\omega)=\begin{cases}\mathrm{sig}(\omega) & \text{if } \omega_{n-1}\le|\omega|\le\omega_n\\ 0 & \text{otherwise}\end{cases} \tag{5}$$

The frequency-domain signal described by Eq. (5) can be transformed into the time domain as

$$c_n(t)=\int_{-\infty}^{\infty}\hat{c}_n(\omega)e^{j\omega t}d\omega=\int_{-\omega_n}^{-\omega_{n-1}}\hat{c}_n(\omega)e^{j\omega t}d\omega+\int_{\omega_{n-1}}^{\omega_n}\hat{c}_n(\omega)e^{j\omega t}d\omega \tag{6}$$

Finally, the original signal sig(t) can be decomposed as

$$\mathrm{sig}(t)=\sum_{n=1}^{N}c_n(t)+\mathrm{noise}(t) \tag{6}$$

where $c_n(t)$ is a mono-component signal with a frequency band of ω_{n-1} ~ ω_n. $c_n(t)$ represents the modal response of a specific mode.

3. Modal parameter identification

Since $c_n(t)$ represents the modal response of a specific structural mode, it can be used to identify the modal parameters of this specific mode. In the following parts of this section, the subscript n is dropped for brevity.

The modal response is a mono-component signal with amplitude modulation and frequency modulation that can be expressed as

$$c(t)=A(t)\cos\left(\int\omega(t)dt+\varphi\right)=A(t)\cos\left(\int 2\pi f(t)dt+\varphi\right) \tag{7}$$

where $A(t)$ is the instantaneous amplitude; $\cos\left(\int 2\pi f(t)dt+\varphi\right)$ is the frequency carrier; $f(t)$ is the instantaneous frequency in Hz; φ is the initial phase.

The instantaneous amplitude can be calculated using the amplitude-modulation and frequency-modulation decomposition proposed in [33]. The instantaneous frequency was usually calculated using the Hilbert transform and some improved variances [33]. However, due to the limitations of the Bedrosian theorem and Nuttall theorem [25], the Hilbert transform-based method sometimes results in large fluctuations and negative values in the calculation result. The empirical envelope method [34] can overcome the limitations of these theorems and therefore results in a better calculation of the instantaneous frequency. Hence, the empirical envelope method is used in this paper to calculate the instantaneous frequency.

The instantaneous logarithmic decrement $\delta(t)$ can be calculated based on the instantaneous amplitude as follows [35]

$$\delta(t_i)=\ln\frac{A(t_i)}{A(t_{i-1})}=\frac{2\pi\xi(t_i)}{\sqrt{1-\xi^2(t_i)}} \tag{8}$$

where i represents the i^{th} time instant; $\xi(t)$ is the instantaneous damping ratio.

For a structural mode with a low damping ratio, the denominator at the right-hand side of Eq. (8) is close to one, and hence $\xi(t)$ can be approximated as [35, 36]

$$\xi(t) = \frac{\ln(A(t_m) / A(t_{m-1}))}{2\pi} \tag{9}$$

For a linear system, the instantaneous frequency and instantaneous damping ratio of each mode are theoretically constant. However, they may fluctuate slightly around a constant value due to the discrete sampling of the signal and the numerical error of the identification method. The constant modal frequency and damping ratio can be calculated as the mean values of the instantaneous frequency and instantaneous damping ratio, respectively. For a time-varying or a nonlinear system, the modal frequency and damping ratio can be identified following the same procedure. However, the instantaneous frequency and instantaneous damping ratio of each mode may vary significantly with time due to the time-varying or nonlinear feature of the system. Finally, it is noted that this study deals with modal parameter identification from impulse excitation-induced responses. If only ambient excitation-induced responses are available, the method can be used together with the random decremental method.

In summary, the proposed modal parameter identification method is outlined as follows: (1) the mono-component modal responses are extracted from the multi-component vibration responses using the EFD method; (2) for each modal response, the instantaneous frequency is identified based on the empirical envelope method; (3) for each modal response, the instantaneous damping ratio is identified based on Eq. (8) and Eq. (9).

4. Numerical examples

Two numerical examples are studied in this section to validate the EFD-based method for modal parameter identifications of structures with closely spaced modes. The superiorities of the EFD-based method relative to the EMD-based method and several other methods are also discussed.

4.1. A linear signal with two closely spaced modes

The first example studies a linear signal with two closely spaced modes described by Eq. (10)

$$c_1(t) = e^{-2\pi\xi_1 f_1 t}\cos\left(2\pi f_1 t\sqrt{1-\xi_1^2}\right) \tag{10a}$$

$$c_2 = e^{-2\pi\xi_2 f_2 t}\cos\left(2\pi f_2 t\sqrt{1-\xi_2^2}\right) \tag{10b}$$

$$\mathrm{sig}_1(t) = c_1(t) + c_2(t) \tag{10c}$$

where f_1 and f_2 are the modal frequencies of $c_1(t)$ and $c_2(t)$, respectively; ξ_1 and ξ_2 are the modal damping ratios of $c_1(t)$ and $c_2(t)$, respectively. The signal sig_1 is a general representation of the free vibration response of a linear two-degree-of-freedom system.

It is first assumed that f_1 = 5.0 Hz, f_2 = 5.4 Hz, $\xi_1 = \xi_2$ = 0.005. These two modes are closely spaced since the differences between f_1 and f_2 are within 10% of their modal frequencies. Fig. 1(a) and Fig. 1(b) show the time-domain and frequency-domain representations of sig_1. The sampling frequency is 1000 Hz and the sampling time is 20 s. A beat phenomenon is observed in Fig. 1(a), which is a typical feature for the free vibration response of a structure with closely spaced modes.

The signal sig_1 is processed by the EFD to extract the modal responses. The decomposition results are presented together with the theoretical modal responses in Fig. 1(c) and Fig. 1(d). It can be seen that the EFD can successfully extract the modal responses from the signal sig_1. The extracted modal responses agree very well with the theoretical modal responses. On the other hand, the EMD is unable to extract the modal responses, as shown in Fig. 2. More specifically, the EMD results in 8 intrinsic mode functions (IMFs). The first intrinsic mode function is close to the sig_1, which is confirmed by their Fourier spectra in Fig. 3. This is because the EMD is unable to separate modal responses with closely spaced modes due to the limited frequency resolution of the EMD. The comparison suggests that EFD has a higher frequency resolution than EMD. Indeed, the EFD performs very well even if $f_2 / f_1 = 1.05$. However, as discussed by Feldman [37], the EMD cannot accurately separate two modes as long as $f_2 / f_1 < 1.50$. In addition, the EMD generates several low-frequency and low-energy pseudo components, which may be confusing in the modal parameter identification for a real structure. The EEMD is also unable to separate the modal responses while the EEMD results are not shown for brevity. It is noted that better results may be obtained by changing the stopping criterion or other parameters of the EMD. However, changing the stopping criterion or other parameters cannot significantly improve the decomposition results due to the limited frequency resolution of EMD. It is also noted that there are some improved EMD-based methods that have better frequency resolution. However, these improved EMD-based methods are developed for specific types of signals, and the improvements in the frequency resolution are often limited. In addition, the computational time of the EFD for the considered signal is about 0.5 seconds, the computational time of the EMD is about 1 second, while the computational time of the EEMD (the ratio of standard deviations between added noise and sig_1 is 0.01, the ensemble number is 1000) is about 24 minutes on a laptop with an i7-8665U CPU, 32.0 GB of RAM, and 64-bit Windows 10. In summary, the EFD has a higher frequency resolution than the EMD and therefore the EFD is more suitable for modal parameter identifications of structures with closely spaced modes.

Fig. 4 shows the instantaneous frequencies and instantaneous damping ratios of sig_1 estimated using the EFD-based method. It can be seen that the estimated results agree very well with the theoretical values. The estimated results fluctuate slightly around the theoretical values, which have been discussed in Section 3. The identified modal parameters and modal damping ratios are listed in Table 1 (i.e., the case with signal-to-noise ratio SNR = + ∞). It can be seen that the identified values are exactly consistent with the theoretical values. The results presented in Fig. 4 and Table 1 convincingly validate the accuracy of the EFD-based method. The EMD is unable to separate the two closely spaced modes and hence the EMD-based method cannot identify the modal parameters of the considered signal.

The accuracy of the EFD-based method is further examined for modal parameter identifications from signals with various single-to-noise ratios (SNRs). More specifically, Gaussian white noise with a zero mean value is added to sig_1. The SNR is defined as $10\log\left(\mathrm{var}\left(\mathrm{sig}_1\right)/\mathrm{var}\left(\mathrm{noise}\right)\right)$, where var represents the variance. The modal parameters identified from signals with various SNRs are listed in Table 1. It can be seen that the identification results agree well with the theoretical values for all considered SNRs. This is due to the robustness of the EFD to noises.

To further examine the identification accuracy of the EFD-based method for signals with closely spaced modes, f_2 is varied and the identification results for different f_2 are presented in Fig. 5. The identification error is defined as $\left(\text{identified value} - \text{theoretical value}\right) / \text{theoretical value}$. It can be seen that the EFD-based method is capable of identifying the modal frequencies of very closely spaced modes with $(f_2 - f_1) / f_1 = 2.0\%$. However, the identification accuracies for the modal damping ratios decrease for very closely spaced modes. The identification errors for the modal damping ratios are within 5% for $(f_2 - f_1) / f_1 > 5.0\%$.

4.2. A nonlinear system with amplitude-dependent frequencies and damping ratios

A two-degree-of-freedom nonlinear system described by Eq. (11) is considered in this example

$$\ddot{c}_1 + 4\pi\left(f_{1,0} - 0.1A_1\right)\left(\xi_{1,0} + 0.01A_1\right)\dot{c}_1 + (2\pi\left(f_{1,0} - 0.1A_1\right))^2 c_1 = 0 \tag{11a}$$

$$\ddot{c}_2 + 4\pi\left(f_{2,0} + 0.1A_2\right)\left(\xi_{2,0} + 0.01A_2\right)\dot{c}_2 + (2\pi\left(f_{2,0} + 0.1A_2\right))^2 c_2 = 0 \tag{11b}$$

$$\text{sig}_2(t) = c_1(t) + c_2(t) \tag{11c}$$

where A_1 and A_2 represent the instantaneous amplitudes of c_1 and c_2, respectively; the overdot indicates the derivative with respect to time t; $f_{1,0}$ = 5.0 Hz and $f_{2,0}$ = 5.4 Hz represent the modal frequencies of the 1st and 2nd modes when the amplitudes are $A_1 = 0$ and $A_2 = 0$, respectively; $\xi_{1,0} = 0$ and $\xi_{2,0} = 0$ are the damping ratios of the 1st and 2nd modes when the amplitudes are $A_1 = 0$ and $A_2 = 0$, respectively. Both modes have modal frequencies and damping ratios that are dependent on the vibration amplitude. The amplitude-dependency of modal parameters is very typical for large-scale civil structures [35, 38, 39]. The two modes are assumed uncoupled and therefore the free vibration response is the summation of the modal responses of the two modes, as shown by Eq. (11c).

Eq. (11) is numerically integrated by a standard Newmark-β method with a sampling frequency of 1000 Hz. The initial conditions are $c_1(t=0) = 1$, $\dot{c}_1(t=0) = 0$, $c_2(t=0) = 1$, and $\dot{c}_2(t=0) = 0$. Time-domain and frequency-domain representations of the free vibration response are depicted in Fig. 6. A beat phenomenon is observed in Fig. 6(a), which is a typical feature for the free vibration response of a structure with closely spaced modes. As can be seen from Fig. 6(b), the signal has two dominant frequencies at around 5 Hz and 5.4 Hz, respectively. However, the Fourier spectra contain no information regarding the nonlinearity of the considered system.

The signal sig_2 is processed by the EFD to extract the modal responses. The decomposition results are presented together with the theoretical modal responses in Fig. 6(c) and Fig. 6(d). It can be seen that the EFD can successfully extract the modal responses from the signal sig_2. The extracted modal responses agree very well with the theoretical modal responses. The computational time of the EFD for the considered signal is less than 0.5 seconds.

Fig. 7 shows the modal frequencies and damping ratios of sig_2 estimated using the EFD-based method. Since the modal frequencies and damping ratios of sig_2 are dependent on the vibration amplitudes, the estimated modal parameters are fitted as amplitude-dependent functions as follows

$$\left(A(t), f(t)\right) \overset{\text{polynomial fitting}}{\rightarrow} f(A) \tag{12a}$$

$$\left(A(t), \xi(t)\right) \overset{\text{polynomial fitting}}{\rightarrow} \xi(A) \tag{12b}$$

It can be seen that the estimated results agree very well with the theoretical values. The estimated results fluctuate slightly around the theoretical values, which have been discussed in Section 3. The results presented in Fig. 7 convincingly validate the accuracy of the EFD-based method for nonlinear systems with closely spaced modes. For comparison, the second example is also identified with the EMD-based method. It is found that the EMD is unable to separate the two closely spaced modes and hence the EMD-based method cannot identify the modal parameters of the considered signal. The EMD results of the considered signal are not shown for brevity.

5. Experimental validation

An experimentally recorded signal sig_3 is considered in this section to validate the accuracy of the EFD-based method. The signal is the acceleration history of a four-story steel structure, which was recorded after the structure was excited by a hammer impact. The structure was designed as the IASC-ASCE structural health monitoring benchmark problem, as shown in Fig. 8. Fig. 9(a) and Fig. 9(b) show the time-domain and frequency-domain representations of sig_3. The sampling frequency is 1000 Hz and the sampling time is 20 s. The Fourier spectrum in Fig. 9(b) suggests that the signal has at least five peaks in the frequency range 0 ~ 22 Hz, with two closely spaced modes around 7.5 Hz.

The signal sig_3 is processed by the EFD to extract the modal responses. The decomposition results are presented in Fig. 9(c) ~ Fig. 9(h). The mean value of c_1 is not zero, indicating that c_1 is not a modal response while it may be induced by the zero-shift of the sensors. c_2 ~ c_6 represent the modal responses of different modes. It can be seen that amplitudes of some components (e.g., c_4) decay exponentially due to damping as expected. On the other hand, the amplitudes of some components (e.g., c_6) do not decay exponentially, which might be due to the existence of measurement noise. Therefore, the modal parameters are identified based on the segments of the modal responses with exponentially decaying amplitude. The instantaneous amplitudes of the utilized segments are highlighted by red lines in Fig. 9(c) ~ Fig. 9(h).

The identified modal parameters are listed in Table 2 together with the results of some previous papers. The modal parameters are also identified based on a standard data-driven stochastic subspace identification (SSI) method [40]. Perez-Ramirez et al. [41] identified the modal parameters using a wavelet transform-based method, which is criticized due to the difficulty to select an appropriate mother wavelet. Yanez-Borjas et al. [42] identified the modal parameters based on the nonlinear mode decomposition, which is also an adaptive decomposition method. However, the computational cost of the nonlinear mode decomposition is much higher than the EFD. More specifically, for the considered signal, the computational time of the EFD is less than 2 seconds, the computational time of the wavelet transform is about 2 minutes, and the computational time of the nonlinear mode decomposition is about 14 minutes on a laptop with an i7-8665U CPU, 32.0 GB of RAM, and 64-bit Windows 10.

The four methods estimate similar results of modal frequencies. However, estimation results for modal damping ratios are quite scattered. This is expected because the damping ratio is sensitive to some

uncertainties like noises and decomposition errors. The results of this example suggest that the EFD-based method can be used for online modal parameter identifications of real structures with closely spaced modes.

6. Conclusion

A new empirical Fourier decomposition (EFD)-based method is proposed for identifying the modal parameters of civil structures from the free vibration responses (which can be obtained from free vibration test or constructed from ambient vibration responses). Three examples are analyzed to show the effectiveness of the proposed method, including a linear signal with closely spaced modes, a nonlinear system with amplitude-dependent frequencies and damping ratios, and a four-story steel structure designed as the structural health monitoring benchmark problem.

The numerical examples show that the EFD-based method has a much higher frequency resolution and lower computational cost than the empirical mode decomposition (EMD)-based method. More specifically, the EFD-based method is capable of identifying the modal frequencies of very closely spaced modes with relative frequency differences of 2.0%, and identification errors for the modal damping ratios are within 5% if the relative frequency difference is larger than 5.0%. For the experimental example, the proposed EFD-based method achieves similar results compared to previous papers using the wavelet transform-based method and nonlinear mode decomposition-based method. However, the computational cost of the EFD-based method is much lower than the other two methods.

References

1. Ramezani, M. and Bahar, O. "Indirect structure damage identification with the information of the vertical and rotational mode shapes", *Scientia Iranica*, **28**, pp. 2101-2118 (2021).
2. Nabavian, S., Davoodi, M., Navayi-Neya, B., et al. "Damping estimation of a double-layer grid by output-only modal identification", *Scientia Iranica*, **28**, pp. 618-628 (2021).
3. Haghi, A. and Rahimi, M. "Control and stability analysis of VSC-HVDC based transmission system connected to offshore wind farm", *Scientia Iranica*, **29**, pp. 193-207 (2022).
4. Shayanfar, M., Hatami, A., Zabihi-Samani, M., et al. "Simulation of the force-displacement behavior of reinforced concrete beams under different degrees and locations of corrosion", *Scientia Iranica*, **29**, pp. 964-972 (2022).
5. Zhang, M., Wu, T., and Øiseth, O. "Vortex-induced vibration control of a flexible circular cylinder using a nonlinear energy sink", *Journal of Wind Engineering and Industrial Aerodynamics*, **229**, p. 105163 (2022).
6. Zhang, M. and Xu, F. "Tuned mass damper for self-excited vibration control: Optimization involving nonlinear aeroelastic effect", *Journal of Wind Engineering and Industrial Aerodynamics*, **220**, p. 104836 (2022).
7. Song, Y., Liu, Z., Rønnquist, A., et al. "Contact wire irregularity stochastics and effect on high-speed railway pantograph–catenary interactions", *IEEE Transactions on Instrumentation and Measurement*, **69**, pp. 8196-8206 (2020).

8. Song, Y., Wang, Z., Liu, Z., et al. “A spatial coupling model to study dynamic performance of pantograph-catenary with vehicle-track excitation”, *Mechanical Systems and Signal Processing*, **151**, pp. 107336 (2021).
9. Wang, Z., Yang, J., Shi, K., et al. “Recent Advances in Researches on Vehicle Scanning Method for Bridges”, *International Journal of Structural Stability and Dynamics*, **22**, p. 2230005 (2022).
10. Yang, Y. and Yang, J. “State-of-the-art review on modal identification and damage detection of bridges by moving test vehicles”, *International Journal of Structural Stability and Dynamics*, **18**, p. 1850025 (2018).
11. Bendat, J. and Piersol, A. “Engineering applications of correlation and spectral analysis”, Wiley Interscience, New York (1980).
12. Gautier, P., Gontier. C., and Smail, M. “Robustness of an ARMA identification method for modal analysis of mechanical systems in the presence of noise”, *Journal of Sound and Vibration*, 1**79**, p. 227-242 (1995).
13. Peeters, B. and De Roeck, G. “Reference-based stochastic subspace identification for output-only modal analysis”, *Mechanical systems and signal processing*, **13**, pp. 855-878 (1999).
14. He, Y., Yang, J., and Li, X. “A three-stage automated modal identification framework for bridge parameters based on frequency uncertainty and density clustering”, *Engineering Structures*, **255**, p. 113891 (2022).
15. Tronci, E., De Angelis, M., Betti, R., et al. “Multi-stage semi-automated methodology for modal parameters estimation adopting parametric system identification algorithms”, *Mechanical Systems and Signal Processing*, **165**, p. 108317 (2022).
16. Mugnaini, V., Fragonara, L., and Civera, M. “A machine learning approach for automatic operational modal analysis”, *Mechanical Systems and Signal Processing*, **170**, p. 108813 (2022).
17. Charbonnel, P. “Fuzzy-driven strategy for fully automated modal analysis: Application to the SMART2013 shaking-table test campaign”, *Mechanical Systems and Signal Processing*, **152**, p. 107388 (2021).
18. Yao, X., Yi, T., Zhao, S., et al. “Fully Automated Operational Modal Identification Using Continuously Monitoring Data of Bridge Structures”, *Journal of Performance of Constructed Facilities*, **35**, p. 04021041 (2021).
19. Kijewski, T., Kareem, A. “Wavelet transforms for system identification in civil engineering”, *Computer - Aided Civil and Infrastructure Engineering*, **18**, pp. 339-355 (2003).
20. Huang, N., Shen, Z., Long, S., et al. “The empirical mode decomposition and the Hilbert spectrum for nonlinear and non-stationary time series analysis”, *Proceedings of the Royal Society of London Series A: mathematical, physical and engineering sciences*, **454**, pp. 903-95 (1998).
21. He, X., Hua, X., Chen, Z., et al. “EMD-based random decrement technique for modal parameter identification of an existing railway bridge”, *Engineering Structures*, **33**, pp. 1348-1356 (2011).
22. Ren, W. and Zong, Z. “Output-only modal parameter identification of civil engineering structures”, *Structural Engineering and Mechanics*, **17**, pp. 429-444 (2004).

23. Fu, C. and Jiang, S. “A Hybrid Method for Structural Modal Parameter Identification Based on IEMD/ARMA: A Numerical Study and Experimental Model Validation”, *Applied Sciences*, **12**, p. 8573 (2022).
24. Rilling, G. and Flandrin, P. “One or two frequencies? The empirical mode decomposition answers”, *IEEE transactions on signal processing*, **56**, pp. 85-95 (2007).
25. Zhang, M. and Xu, F. “Variational mode decomposition based modal parameter identification in civil engineering”, *Frontiers of Structural and Civil Engineering*, **13**, pp. 1082-1094 (2019).
26. Wu, Z. and Huang, N. “Ensemble empirical mode decomposition: a noise-assisted data analysis method”, *Advances in adaptive data analysis*, **1**, pp. 1-41 (2009).
27. Torres, M., Colominas, M., Schlotthauer, G., et al. “A complete ensemble empirical mode decomposition with adaptive noise”, *IEEE international conference on acoustics, speech and signal processing (ICASSP): IEEE*, New York, pp. 4144-4147 (2011).
28. Dragomiretskiy, K. and Zosso, D. “Variational mode decomposition”, *IEEE transactions on signal processing*, **62**, pp. 531-544 (2013).
29. Iatsenko, D., McClintock, P., and Stefanovska, A. “Nonlinear mode decomposition: a noise-robust, adaptive decomposition method”, *Physical Review E*, **92**, p. 032916 (2015).
30. Zhou, W., Feng, Z., Xu, Y., et al. “Empirical Fourier decomposition: An accurate signal decomposition method for nonlinear and non-stationary time series analysis”, *Mechanical Systems and Signal Processing*, **163**, p. 108155 (2022).
31. Zubaydi, A., Haddara, M., and Swamidas, A. “On the use of the autocorrelation function to identify the damage in the side shell of a ship's hull”, *Marine Structures*, **13**, pp. 537-51 (2000).
32. Ibrahim, S. “Random decrement technique for modal identification of structures”, *Journal of Spacecraft and Rockets*, **14**, pp. 696-700 (1977).
33. Huang, N., Wu, Z., Long, S., et al. “On instantaneous frequency”, *Advances in adaptive data analysis*, **1** pp. 177-229 (2009).
34. Zheng, J., Cheng, J., and Yang, Y. “A new instantaneous frequency estimation approach-empirical envelope method”, *Zhendong yu Chongji(Journal of Vibration and Shock)*, **31**, pp. 86-90 (2012).
35. Zhang, M. and Xu, F. “Nonlinear vibration characteristics of bridge deck section models in still air”, *Journal of Bridge Engineering*, **23**, p. 04018059 (2018).
36. Chopra, A. Dynamics of structures, Pearson Education, India (2007).
37. Feldman, M. “Analytical basics of the EMD: Two harmonics decomposition”, *Mechanical Systems and Signal Processing*, **23**, pp. 2059-2071 (200).
38. Zhang, M., Xu, F., and Han, Y. “Assessment of wind-induced nonlinear post-critical performance of bridge decks”, *Journal of Wind Engineering and Industrial Aerodynamics*, **203**, p. 104251 (2020).
39. Ge, X. and Yura, J. The strength of rotary-straightened steel columns. *Proceedings-Annual Stability Conference*, SSRC, St Louis, pp. 425-442 (2019).
40. Alıcıoğlu, B. and Luş, H. “Ambient vibration analysis with subspace methods and automated mode selection: case studies”, *Journal of Structural Engineering*. **134**, pp. 1016-1029 (2008).

41. Perez-Ramirez, C., Amezquita-Sanchez, J., Adeli, H., et al. “New methodology for modal parameters identification of smart civil structures using ambient vibrations and synchrosqueezed wavelet transform”, *Engineering Applications of Artificial Intelligence*, **48**, pp. 1-12 (2016).
42. Yanez-Borjas, J., Amezquita-Sanchez, J., Valtierra-Rodriguez, M., et al. “Nonlinear mode decomposition-based methodology for modal parameters identification of civil structures using ambient vibrations”, *Measurement Science and Technology*, **31**, p. 015007 (2019).

List of figure and table captions

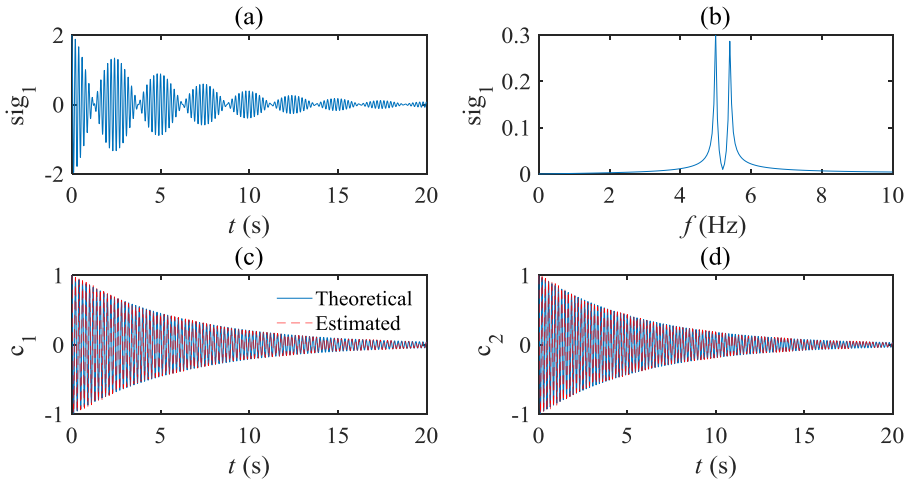

Fig. 1. A linear signal sig_1 with two closely spaced modes and EFD results.

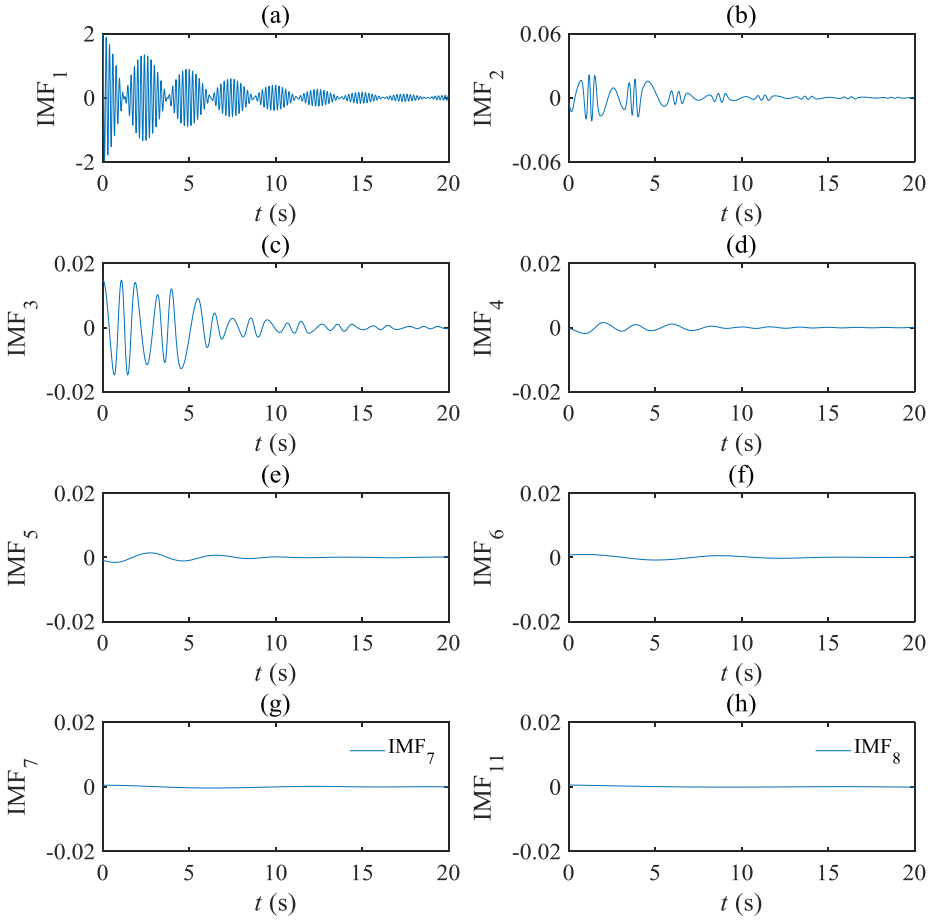

Fig. 2. EMD results of a linear signal sig_1 with two closely spaced modes.

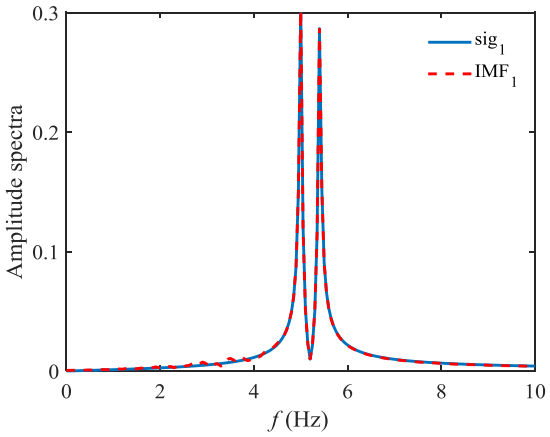

Fig. 3. Fourier spectra of sig_1 and the first intrinsic mode function.

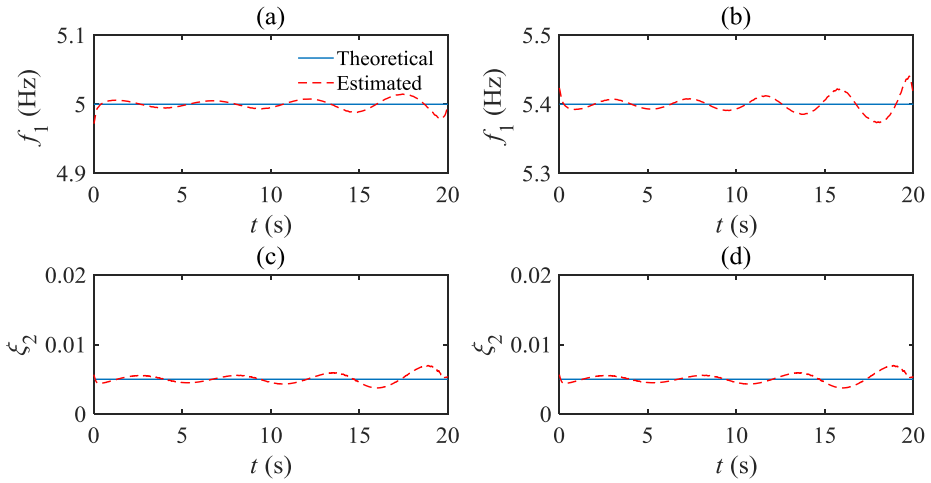

Fig. 4. Instantaneous frequencies and instantaneous damping ratios of a linear signal sig_1 with two closely spaced modes.

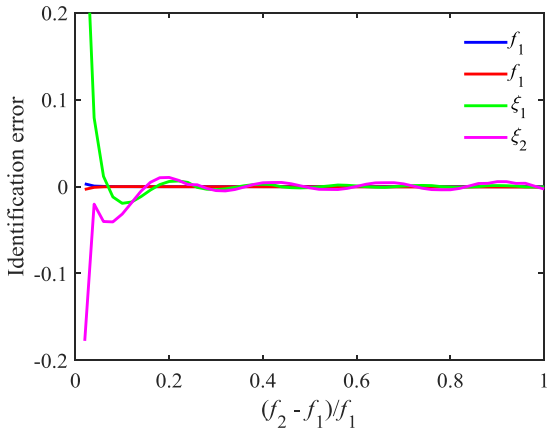

Fig. 5. Identification results of modal parameters from signals with various f_2.

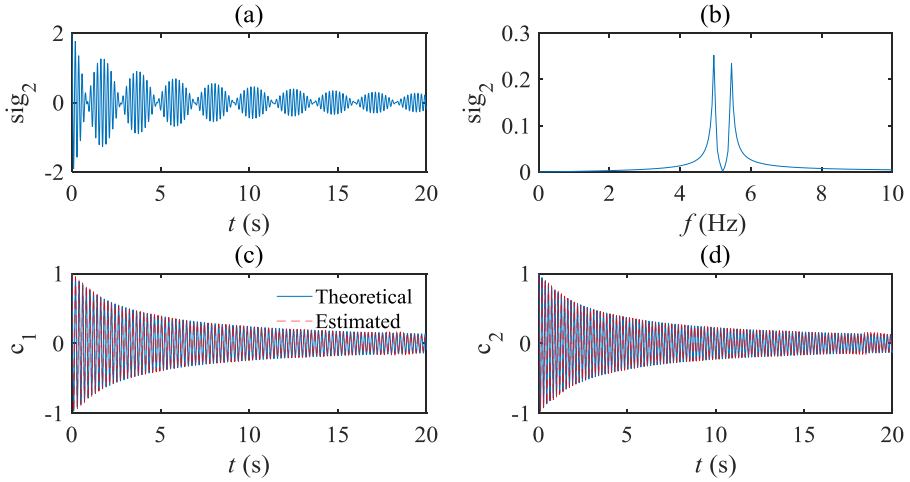

Fig. 6. Free vibration response of a two-degree-of-freedom nonlinear system and EFD results.

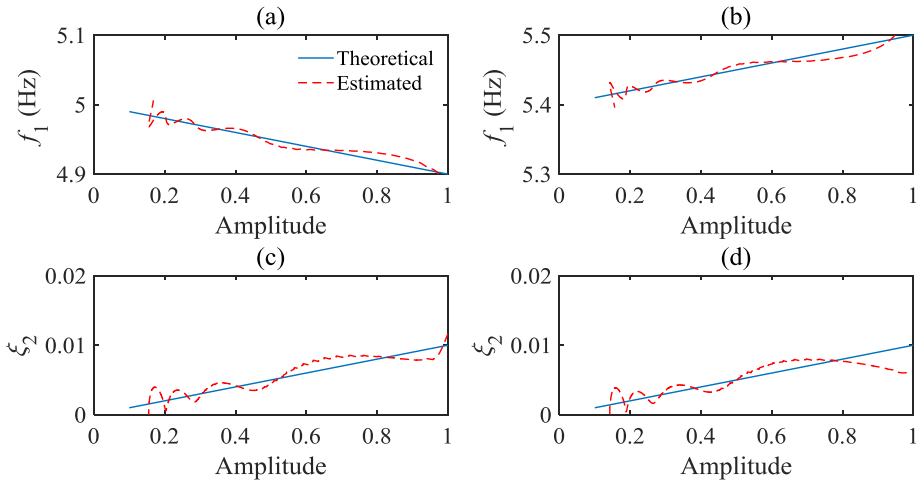

Fig. 7. Amplitude-dependent frequencies and damping ratios of a two-degree-of-freedom nonlinear system.

Fig. 8. Structure for IASC-ASCE structural health monitoring benchmark problem.

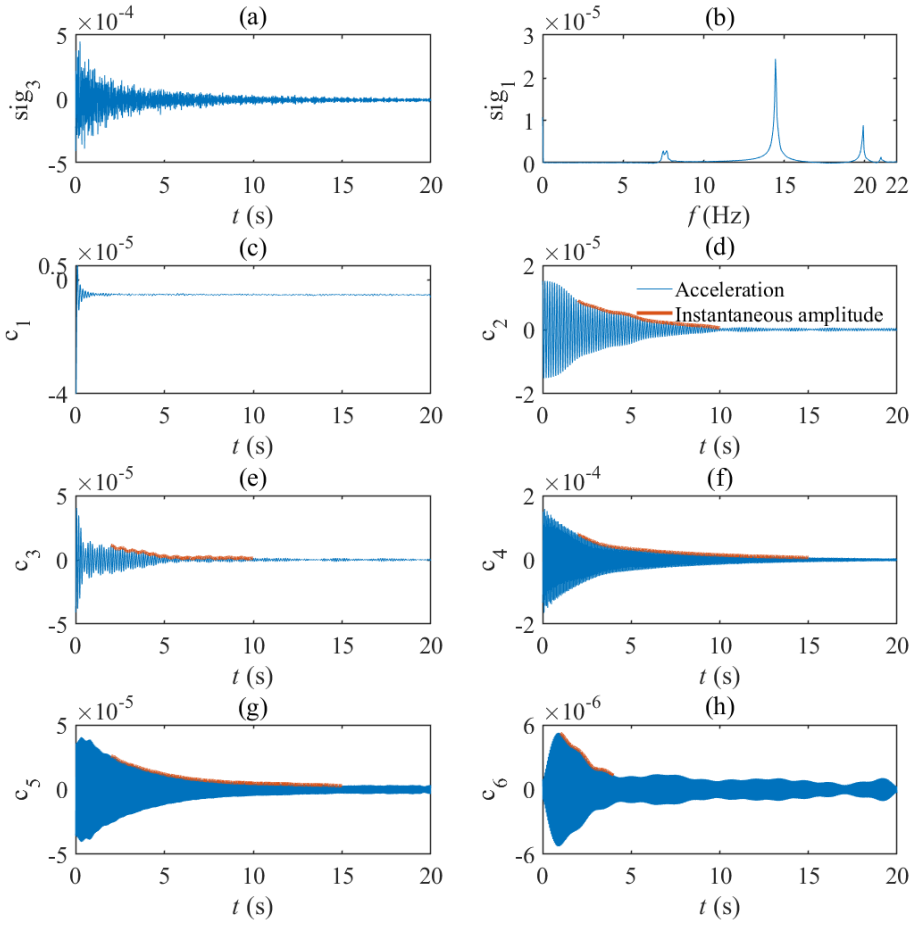

Fig. 9. Free vibration response of a four-story steel structure and EFD results.

Table 1. Identification results of modal parameters from signals with various SNRs.

SNR (dB)	f_1 (Hz)	f_2 (Hz)	ξ_1 (%)	ξ_2 (%)
$+\infty$	5.00	5.40	0.50	0.50
40	5.00	5.40	0.50	0.50
30	5.00	5.40	0.50	0.50
20	5.00	5.40	0. 49	0.48
10	4.97	5.40	0.51	0.48

Table 2. Identification results of modal parameters for a four-story steel structure.

Mode number	f (Hz)	ξ (%)	f (Hz)	ξ (%)	f (Hz)	ξ (%)	f (Hz)	ξ (%)
	EFD-based method		SSI [40]		Yanez-Borjas et al. [42]		Perez-Ramirez et al. [41]	
1	7.50	0.770	7.49	0.86	7.48	0.552	7.47	0.87
2	7.70	0.555	7.76	0.74	7.77	0.426	7.77	0.79
3	14.45	0.021	14.49	0.15	14.48	0.114	14.51	0.11
4	19.89	0.013	19.89	0.00	19.89	0.003	19.88	0.00
5	20.99	0.034	21.01	0.04	21.02	0.045	21.01	0.08

Biographies

Shimin Li is a researcher at the Guiyang Yunyan District Municipal Engineering Management Office, Guiyang, China. His main research fields include structural dynamics and modal parameter identification. Recently he is mainly working on modal parameter identification of bridge structures.

Yuelong Liu is an engineer at the Guiyang Yunyan District Municipal Engineering Management Office, Guiyang, China. His main research fields include structural dynamics and modal parameter identification. Recently he is mainly working on modal parameter identification of bridge structures.

Pengcheng Wang is an engineer at the Guizhou Construction Science Research & Design Institute Limited Company of CSCEC, Guiyang, China. His main research fields include structural dynamics and modal parameter identification. Recently he is mainly working on structural dynamics of bridge structures.

Xian Li is an engineer at the Guizhou Gongda Science and Technology Service Co. LTD, Guiyang, China. His main research fields include structural design and modal parameter dynamics. Recently he is mainly working on structural design of bridge structures.

Zhengwei Li is an engineer at the Guizhou Gongda Science and Technology Service Co. LTD, Guiyang, China. His main research fields include structural design and structural dynamics. Recently he is mainly working on structural design of bridge structures.